FIRST NUMERICAL RESULTS ON FORCED-CONVECTION HEAT TRANSFER INSIDE A RECTANGULAR CHANNEL WITH STRAIGHT RIBS ON LOWER AND UPPER WALLS

L.Marocco, D.Fustinoni, P.Gramazio, A.Niro

Dipartimento di Energia, Politecnico di Milano
Campus Bovisa, via Lambruschini, 4 – 20156 Milano, Italy

alfonso.niro@polimi.it

ABSTRACT
This paper presents the first results of a numerical investigation on the fluid dynamics and heat transfer characteristics of a forced air-flow inside a rectangular channel with straight ribs on the lower and upper walls. The Reynolds number is 4180. The upper and lower walls are maintained at constant temperature whereas the side walls are adiabatic. The duct is 120 mm wide, 12 mm height and 840 mm long. The ribs have a square cross section of 4 mm^2 and are 20 mm spaced. The calculations are carried out with a commercial code using a RANS approach with different turbulence models. A two-dimensional numerical analysis is performed on the entire fluid domain. The average heat transfer coefficient over the entire channel and the pressure drops are compared with the measured values from an experimental facility with the same geometry and operating conditions as the numerical model.

1. INTRODUCTION

Turbulence promoters in form of ribs are commonly used in various equipment such as turbine cooling channels, heat exchangers, nuclear reactors and solar air heaters. This artificial roughness surfaces modify the fluid dynamics by various mechanisms, such as periodic interruption of the boundary layer growth or periodic streamline deflection and in addition they promote turbulence development as their characteristic size is close to the turbulent microscales (the lower the Reynolds number, the larger the size of dissipative structures).

The authors are currently involved in an investigation on fluid dynamics and heat transfer characteristics of forced convection inside periodic ribbed channels of various configurations [1]. Scope of this work is to examine the performance of the four turbulence models (k-ε realizable, k-ε RNG, k-ω standard, k-ω SST) in predicting the heat transfer coefficient and pressure drops in a rectangular channel with staggered straight ribs mounted on the top and bottom wall under constant wall temperature conditions and for a Reynolds number of 4180 by comparison with data of an experimental facility operated under the same conditions.

2. PROBLEM CONFIGURATION

The solution domain is illustrated in Fig.1 and is summarized in Table 1 together with the thermophysical properties of the flowing air. It reflects the geometry of the experimental facility except for the entrance and exit channels from the test section, which are shorter, having a length of 20H and 10H respectively to ensure a fully developed turbulent flow at inlet and to avoid end effects, respectively.

Although there is experimental evidence of the presence of secondary flows on the rear side of the ribs [2], these are weak and their influence on the heat transfer is negligible allowing to consider the problem as two-dimensional.

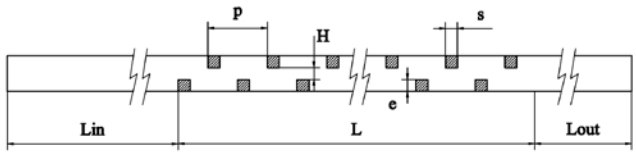

Figure 1: Computational domain of the ribbed channel

Table 1: Channel and ribs configuration according to Fig.1; Thermophysical properties of fluid and flow conditions.

Geometry	
Channel clear height, H	8 mm
Width, W	120 mm = 15H
Length of test section, L	840 mm =105H
Inlet duct length, L_{in}	160 mm = 20H
Outlet duct length, L_{out}	80 mm = 10H
Rib height, e	2 mm = 0.25H
Rib width, s	2 mm = 0.25H
Length of period, p	20 mm = 2.5H; p/e = 10
Number of ribs on each surface	42
Hydraulic diameter, D_h	16 mm = 2H
Thermophysical properties	
Fluid	Air
Ambient temperature, T_0	22.73°C
Ambient pressure, P_0	101325 Pa
Density @ T_0, ρ	1.193 kg/m³
Dynamic viscosity, ν	1.85 10^{-5} Pa s
Specific heat @ T_0, c_p	1005 J/kgK
Thermal conductivity, k	0.0262 W/mK
Flow conditions	
Mass flow rate	0.00928 kg/s
Mean inlet velocity	5.4 m/s
Reynolds number, $\frac{UD_h}{\nu}$	4180

The numerical simulations have been performed according to the following assumptions:

- Two-dimensional fluid flow and heat transfer;
- Fully turbulent and incompressible flow;
- Body forces and viscous dissipation are neglected;
- Radiation heat transfer is neglected;
- Constant thermophysical properties.

The last assumption is justified by the small bulk temperature increase of approximately 14°C across the heated length of the test section.

3. PROBLEM SETUP

3.1 Boundary conditions

The fluid enters the channel at ambient temperature T_0 and with a uniform velocity, U=5.4 m/s, calculated from the measured value of volume flow rate. The inlet turbulence intensity is set at a value of 10%. The upper and lower plates are maintained at a constant temperature T_w=40°C while the wooden ribs are considered adiabatic. No-slip boundary conditions are enforced at all walls and rib sides. The outlet pressure equals the atmospheric pressure.

3.2 Turbulence models

The heat transfer enhancement and thermal performance in a channel with ribs in different geometries and arrangements has been already numerically studied but different authors do not agree about the best turbulence model to be used. Wongcharee et al. [3] compared the numerical results obtained with the k-ε RNG and k-ω SST turbulence models with the experimental data of Kilicaslan et al. [4] and concluded that the k-ω SST model works better. Chaube et al. [5] performed a similar study by comparing the heat transfer prediction in the inter-rib region with the experimental results of Tanda [6]. They tested the k-ε realizable, k-ε RNG, k-ω standard and k-ω SST and this last gave the best results. Eiamsa-ard et al. [7] simulated numerically the experimental facility of Lorenz et al. [2] using four different turbulence models, i.e. k-ε standard, k-ε RNG, k-ω standard and k-ω SST and best agreement was obtained with the standard k-ε and k-ε RNG models.

Therefore, the present study has been performed using the most promising four different turbulence models:

- k-ε realizable
- k-ε RNG
- k-ω standard
- k-ω SST

For the k-ε models the so called “enhanced wall functions” are used, resolving the viscosity-affected near-wall region all the way down to the viscous sublayer.

3.3 Numerical simulation method

The time-averaged continuity, momentum, energy and turbulence equations are solved numerically, sequentially (Pressure based solver), by a finite volume method using the commercial CFD code ANSYS FLUENT v.13. The SIMPLE algorithm is used for the pressure-velocity coupling and a second order scheme for the spatial and temporal discretization. In order to check the possibility of a periodic solution due to the vortex shedding behind the ribs, an unsteady, transient problem has been solved.

A convergent solution is considered to be reached when the following conditions are satisfied:

- constant average drag coefficient on the channel walls;
- constant average heat transfer coefficient;
- normalized residual values lower than 10^{-7} for all variables.

As shown in Fig.2, a non-uniform and partly non-conformal rectangular mesh has been used in order to capture the sharp gradients near the fluid-solid interfaces and to maintain a value of $y^+\approx1$ to resolve the laminar sub-layer without getting too many cells in the core flow region. Successive grid refinements have been done to obtain a grid independent solution. The results discussed in this paper refer to a domain discretization with 368 000 elements.

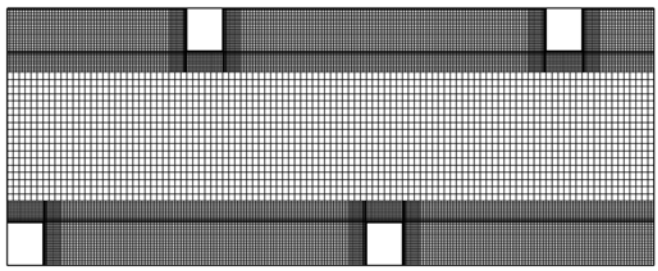

Figure 2: Rectangular non-conformal mesh of the typical computational domain; 368000 cell elements.

4. RESULTS

4.1 Flow structure

According to the velocity contours in Fig. 3, for the remainder of this work the only distinction will be made between k-ε Realizable and k-ω SST turbulence model, giving the k-ε Realizable and k-ε RNG and the k-ω standard and k-ω SST identical results.

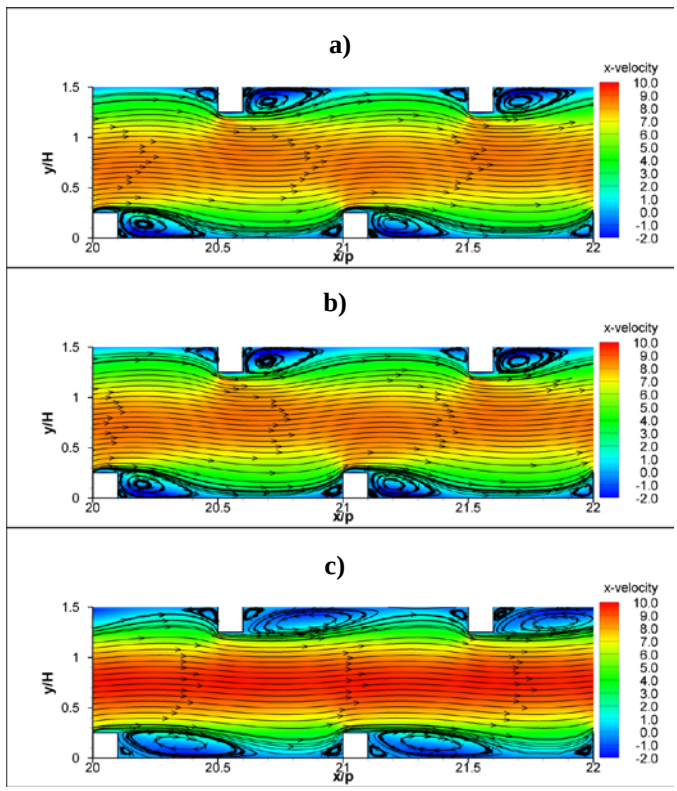

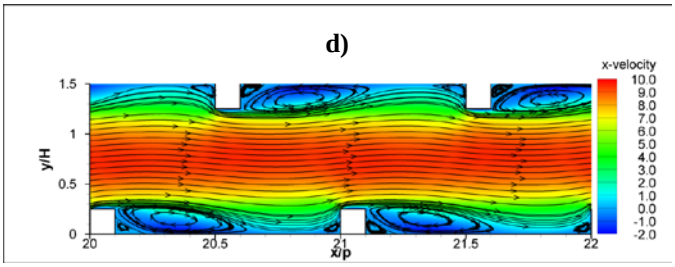

Figure 3: Contour plots of x-velocity of periodic flow with a) k-ε Realizable; b) k-ε RNG; c) k-ω Standard; d) k-ω SST.

A clockwise recirculating vortex in the low pressure region between two ribs is always predicted. Anyway the k-ε models show a shorter and weaker vortex than the k-ω models.

The core streamlines of the k-ε models show a higher deflection from a straight line indicating a better fluid mixing within the channel.

The plot of the x-velocity gradient with respect to the normal wall coordinate gives the position of the reattachment point of the flow. Indeed at the separation point du/dy becomes zero and decreases until it increases again becoming again zero where the flow reattaches (Fig.4).

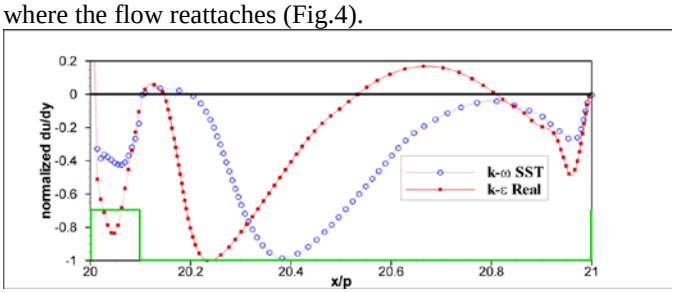

Figure 4: Normalized x-velocity gradients on the bottom wall of the ninth period.

The k-ε models predict a reattachment of the main flow to the bottom wall in the inter-rib region while no reattachment is predicted by the k-ω models. This is also reflected in the contour plots where the core velocity obtained with the k-ω SST is sensibly higher because of the free area reduction.

4.2 Heat transfer

The average Nusselt number over a length equal to pitch p is defined as:

$$Nu_i = \frac{h_i d_h}{k} \qquad (1)$$

where the period's heat transfer coefficient, h_i, is:

$$h_i = \frac{\dot{m} c_p}{2(p-s)W} \ln\left(\frac{T_w - T_{b,i}}{T_w - T_{b,i+1}}\right) \qquad (2)$$

The average Nusselt number, Nu_m, over the entire channel length is the arithmetic average of N periods:

$$Nu_m = \frac{1}{N}\sum_{1}^{N} Nu_i \qquad (3)$$

The temperature $T_{b,i}$ and $T_{b,i+1}$ in the definition of Eq. 2 are the bulk temperatures at the inlet and outlet of the i-th period, respectively. In order to verify the thermal periodicity, i.e. $Nu_i = Nu_{i+1}$, the mean Nusselt numbers over the periods are plotted in Fig. 5. Periodic thermal conditions are assumed to be reached when the difference between the mean Nusselt numbers of two consecutive periods is less than 1%. This condition is satisfied after twelve periods with the k-ω SST model and only six periods with the k-ε realizable model. Furthermore the asymptotic mean Nusselt number is substantially different for the two models, i.e. $Nu_{m,k\varepsilon}$=38.4 and $Nu_{m,k\omega}$=44.7.

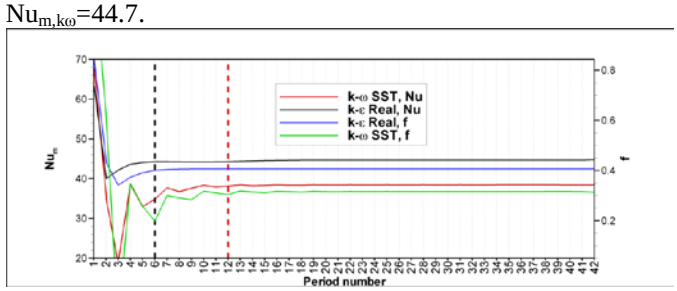

Figure 5: Mean Nusselt number over the periods.

The explanation of the initial decrease and successive monotonically increase of the Nusselt number and the friction factor can be explained by observing the reattachment point of the main flow to the bottom wall, as illustrated in Fig. 6.

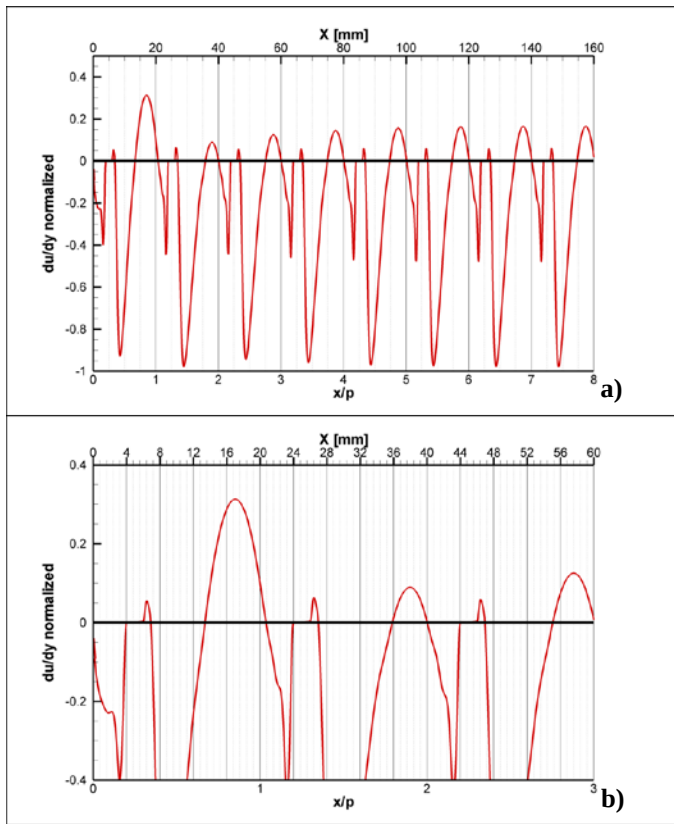

Figure 6: Normalized x-velocity gradients on bottom wall for the k- ε model; a) 1-6 periods; b) 1-3 periods.

The flow reattachment in the second period occurs at a position closer to the front flank of the successive ribs than in the first period. This implies the existence of a broader recirculation zone and thus a thicker boundary layer, causing a reduction in heat transfer and friction factor. From the third period on, the reattachment point moves towards the rear flank of the preceding rib but never reaches the reattachment position of the first period. Therefore the Nusselt number and friction factor increase up to their asymptotic values.

The turbulence intensity distribution, Fig. 7, highlights the position of the peaks downstream of the ribs and the higher values predicted with the k-ε realizable model that contribute to a better heat transfer and therefore to a higher mean Nusselt number.

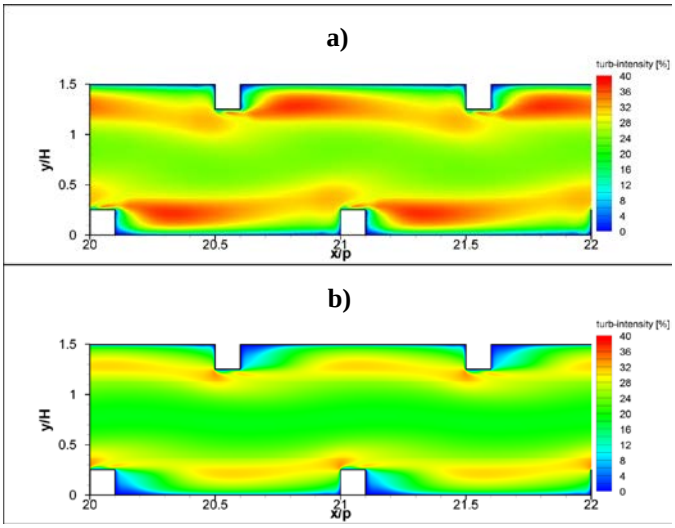

Figure 7: Turbulence intensity distribution; a) k-ε realizable; b) k-ω SST.

The large recirculation zone between two adjacent ribs obtained with the k-ω SST is responsible for the low turbulence intensity and a thicker boundary compared to the k- ε realizable model, as illustrated in the temperature distribution of Fig. 8. Hot spots exist close to the rear side of the ribs, attributed to the poor heat transfer from the wall to the fluid due to the recirculation zone there. This effect is more evident for the k-ω SST model, where the vortex fills the entire region between two adjacent ribs.

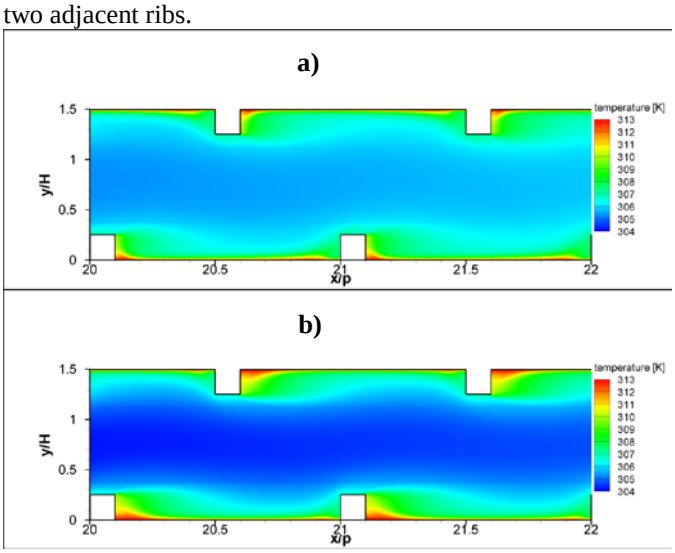

Figure 8: Temperature distribution; a) k-ε realizable; b) k-ω SST.

5. Conclusions

Table 2 summarizes the pressure drops and Nusselt numbers between test section inlet and outlet obtained with the numerical simulations with the experimental measurement of Fustinoni et al. [9], who used in their definitions of Reynolds and Nusselt a characteristic reference length of 0.021m.

Table 2: Pressure drops between test section inlet and outlet

	ΔP [Pa]	**Δ [%]**	**Nu**	**Δ [%]**
k-ε realizable	387.3	10.4	44.8	-27.0
k-ω SST	303.4	-13.4	38.3	-37.5
Experimental	351.0	-	61.3	-

Certainly the hypothesis of adiabatic ribs contributes to the lower numerical value of the Nusselt number compared to the experiment.

The k-ω SST model underpredicts both pressure drops and Nusselt number, coherently with the Reynolds analogy. This is not true for the k-ε realizable model, which overpredicts the pressure drops and underpredicts the Nusselt number.

Furthermore, there is experimental evidence of reattachment at the bottom between the ribs for a pitch-to-height ratio, p/e, greater than 6 [8], which is here reproduced only by the k-ε realizable model, which seems therefore to be more appropriate for the study of turbulent convective flows inside ribbed channels. The discrepancy between the numerical results and the experimental data needs a further detailed analysis that is currently ongoing. This also include the simulation of a three-dimensional domain using LES in order to investigate the presence of secondary flows close to the rear flank of the ribs [2].

NOMENCLATURE

Symbol	Quantity	SI Unit
f	Friction factor, $f = \frac{(\Delta P / p) d_h}{0.5 \rho U^2}$	
h	Heat transfer coefficient	W/m^2K
$\dot{m}$	Mass flow rate	kg/s
Nu	Nusselt number	

REFERENCES

[1] R. Mereu, E. Colombo, F. Inzoli, A. Niro, First numerical results on forced-convection heat transfer inside a wavy channel, *Proc. ThermaComp*, Naples, Italy, 2009.

[2] S. Lorenz, D. Mukomilow, W. Leiner, Distribution oft he heat transfer coefficient in a channel with periodic transverse grooves, *Exp. Therm. and Fluid. Sci.*, vol. 11, pp. 234-242, 1995.

[3] K.Wongcharee, W. Changcharoen, S. Eiamsa-ard, Numerical investigation of flow friction and heat transfer in a channel with various ribs mounted on two opposite ribbed walls, *Int, Jou. of Chem. Reactor Eng.*, vol. 9, A26, 2011.

[4] I.Kilicaslan, H,I. Sarac, Enhancement of heat transfer in compact heat exchanger by different type of rib with holographic interferometry, *Exp. Thermal and Fluid Sci*, vol. 17, pp. 339-346, 1998..

[5] A.Chaube, P.K. Sahoo, S.C. Solanki, Analysis of heat transfer augmentation and flow characteristics due to rib roughness over absorber plate of a solar air heater, *Renewable Energy*, vol. 31, pp. 317-331, 2006.

[6] G. Tanda, Heat transfer in rectangular channel with transverse and V-shaped broken ribs, *Int. Jou. of Heat and Mass Transfer*, vol. 47, pp. 229-243, 2004.

[7] S. Eiamsa-ard, P. Promvonge, Numerical study on heat transfer of turbulent channel flow over periodic grooves, *Int. Comm. in Heat and Mass Transfer*, vol. 35, pp. 844-852, 2008.

[8] S. Okamoto, K. Nakaso, Turbulent shear flow over rows of two-dimensional square ribs on ground plane, *Eigth Symp. Turbulent shear flows*, Technical University of Munich, Germany, 1991.

[9] D. Fustinoni, P. Gramazio, A. Niro, *Heat transfer characteristics in forced convection through a rectangular channel with ribbed surfaces*, UIT conference, Torino, 2011.